UDC 629.5.028.722:531:678.6

Ivan ĆATIPOVIĆ
Većeslav ČORIĆ
Jadranka RADANOVIĆ

An Improved Stiffness Model for Polyester Mooring Lines

Original scientific paper

The stiffness model of highly extensible polyester mooring lines is studied. Mooring lines are considered within coupled dynamic model of a moored floating object. In more detail, deepwater mooring with taut polyester mooring lines is observed. In this case mooring line is modelled as an extensible cable without bending and torsional stiffness. Movements are assumed to be three-dimensional, so it is necessary to examine large displacement model. In longitudinal strain calculation the material of the mooring line is considered as nonlinear. A large elongation value is examined within the stiffness model. Inertial forces of the mooring line are also considered. Hydrodynamic loads due to surrounding fluid are taken into account with the Morison equation. Due to nonlinear properties of mooring lines calculations have to be done in time domain. On these assumptions, derivation of a mooring line finite element is presented for static and dynamic analysis. A floating object is modelled as a rigid body with six degrees of freedom and with small displacements assumption. Hydrodynamic coefficients are calculated in a specified frequency domain; therefore, mapping from the frequency to the time domain is necessary. Comparison between the improved model developed in this paper and current equivalent model is done. A simple mooring line that can be analytically described was the base for comparison. The improved model achieved better agreement with the analytical result.

Keywords: *coupled model, dynamic response, finite element method, large elongation value, mooring,time domain, polyester rope*

Poboljšani model krutosti poliesterskih sidrenih linija

Izvorni znanstveni rad

U članku se proučava model krutosti jako rastezljivih sidrenih poliesterskih linija. Sidrene linije razmatraju se unutar spregnutog modela koji opisuje usidreni plutajući objekt. Iscrpnije, razmatra se sidreni sustav s nategnutim sidrenim linijama od poliestera za sidrenje na velikim dubinama. U ovom slučaju sidrena se linija modelira kao rastezljivo uže bez savojne i torzijske krutosti. Pretpostavlja se da su gibanja trodimenzionalna, stoga treba ispitati model s velikim pomacima. Kod proračuna uzdužne deformacije uzima se u obzir nelinearnost materijala sidrene linije. Visoki iznos istezanja razmatra se u okviru modela krutosti. Inercijske sile koje djeluju na sidrenu liniju također se uzimaju u obzir. Hidrodinamička opterećenja koja nastaju zbog okolnoga fluida proračunavaju se pomoću Morisonove jednadžbe. Zbog nelinearnih značajki sidrenoga sustava svi proračuni se moraju provesti u vremenskoj domeni. Na osnovi navedenih pretpostavki prikazan je izvod konačnog elementa sidrene linije za statički i dinamički slučaj. Plutajući objekt razmatra se kao kruto tijelo sa šest stupnjeva slobode i uz pretpostavku malih pomaka. Hidrodinamički koeficijenti prvo se proračunavaju u frekvencijskoj domeni, a zatim se provodi preslikavanje iz frekvencijske u vremensku domenu. Provedena je usporedba između poboljšanog modela koji je razvijen u ovom radu i jednoga suvremenog modela. Osnova za usporedbu jedna je sidrena linija za koju se mogu dobiti analitički rezultati. Poboljšani model postigao je bolje slaganje rezultata s analitičkim modelom.

Ključne riječi: *dinamički odziv, rastezljivost, poliestersko uže, sidrenje, spregnuti model, metoda konačnih elemenata, vremenska domena*

Authors' Address (Adresa autora):
University of Zagreb, Faculty of Mechanical Engineering and Naval Architecture
Ivana Lučića 5, 10 000 Zagreb, Croatia
E-mail: ivan.catipovic@fsb.hr

Received (Primljeno): 2011-03-08
Accepted (Prihvaćeno): 2011-04-12
Open for discussion (Otvoreno za raspravu): 2012-10-01

1 Introduction

Polyester mooring lines endure high elongation during exploitation. Breaking point can be usually found at 15% elongation. Taut polyester lines can form a part of deep-water mooring solution. The characteristics of such mooring system are significantly influenced by extensibility of polyester rope. The stiffness of mooring system is especially sensitive to elongation of mooring lines. A part of this problem is nonlinear stress-strain relation of polyester fibres.

A coupled dynamic model is recommended way to solve a deep-water mooring problem. This model is composed of dynamics of mooring lines and a floating body dynamics. Inertial and restoring forces of the mooring line as well as hydrodynamic loads are examined. Dynamics of the floating body incorporates environmental loads such as: wave loads of the first and the second order, wind loads and sea current loads. Added mass, damping due to wave radiation and due drag resistance as well as hydrostatic forces are also considered. It should be noted that

the coupled model is solved in the time domain because of the nonlinear properties of mooring system.

Elastic rod theory is a cornerstone for the mooring line dynamics in this study. This theory was derived by Nordgen [1] and Garrett [2]. Nordgen described equation of large motions of elastic rod in terms of centreline position. Garrett incorporated large strain assumptions and suggested finite element method (FEM) for numerical calculation. Three papers concerning coupled dynamics of moored vessel attracted special attention of ISSC 2006 Technical Committee 1.2. [3]. Tahar & Kim [4] developed a computer program for hull/mooring/riser coupled dynamic analysis of a tanker based turret-moored FPSO. Garrett [5] performed a fully coupled global analysis of floating production system, including the vessel, the mooring and the riser system. Kim et al. [6] solved simultaneously the vessel and mooring line dynamics. The vessel global motions and mooring tension were tested at the wave basin of *Offshore Technology Research Center* (Texas, USA) for the non-parallel wind-wave-current 100-year hurricane condition in the Gulf of Mexico. Stiffness nonlinearity of polyester mooring cables was studied by Fernandes et al.[7]. They examined acceptance tests performed with actual full scale cables. As a result they suggested a formula for specific modulus of polyester ropes in terms of dynamic analysis. Tjavaras et al. [8] studied numerically the mechanics of highly extensible cables. In this model a nonlinear stress-strain relation is employed. Numerical solution was based on finite difference scheme. Tahar & Kim [9] examined coupled dynamics analysis of floating structures with polyester mooring lines. Their mathematical model allowed relatively large elongation of polyester rope and nonlinear stress-strain relationship. The mooring line dynamics was based on elastic rod theory. Numerical calculations are done utilizing nonlinear FEM.

A novel procedure for the polyester mooring lines is presented in the paper. This procedure has an improved approximation of the mooring line stiffness, taking into account nonlinear tension-elongation relationship. Development of the procedure is done within the coupled dynamic analysis of the moored vessel. Therefore, a new kind of the coupled dynamic model is formed and it can be used for better evaluation of highly extensible polyester mooring lines.

2 Mathematical model

2.1 Dynamics of the mooring line

Elastic rod theory [1],[2] is a cornerstone for the mathematical model. The behaviour of a slender rod is expressed in terms of the centreline position. Movements are three-dimensional, so it is necessary to examine large displacement model. High elongation value of the mooring line is considered for the modelling of the stiffness. Nonlinearity of tension-elongation relationship is taken into account. The cross-section is assumed to be homogeneous and circular. Bending and torsional stiffness are neglected as well as shear deformation and rotary inertia terms. Governing equations are treated in global coordinate system, so there is no need for any kind of coordinate system transformation.

2.1.1 Motion equation

The centreline of a deformed rod is described by a space curve [10]. In governing equations the space curve is defined by a position vector **r**. Any point on the curve is defined by an arc-length of the extended rod $\tilde{s}$. In this case, a unit tangent vector of the space curve is given as

$$\mathbf{u} = \frac{\mathrm{d}\mathbf{r}}{\mathrm{d}\tilde{s}} \tag{1}$$

with

$$|\mathbf{u}| = 1. \tag{2}$$

Within dynamic analysis the position vector **r** is also function of the time *t*. A segment of the mooring line is shown in n Figure 1 where:

$\tilde{s}$ – arc-length of the extended mooring line
F – cross-section internal force
q – distributed load
p – hydrostatic pressure of the sea water
$\tilde{m}$ – distributed mass of the extended mooring line
$\ddot{\mathbf{r}}$ – acceleration of the segment.

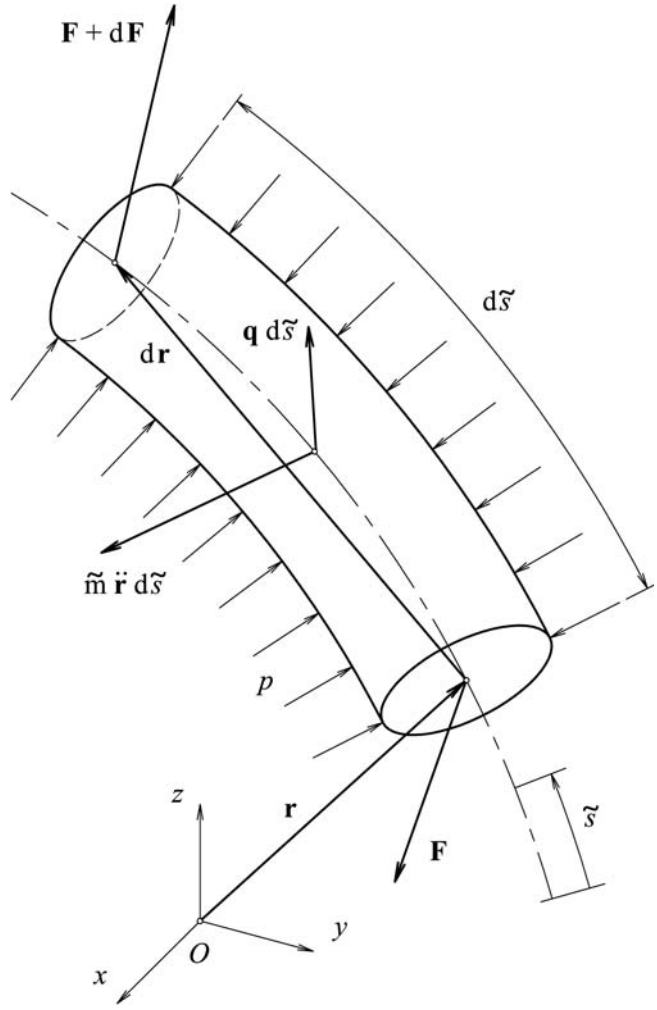

Figure 1 **Segment of the mooring line**
Slika 1 **Diferencijalni element sidrene linije**

Archimedes' principle states that the buoyancy force exerted on an object completely enclosed by a fluid is equal to the weight

of the fluid displaced by the object. The segment of the mooring line is not completely enclosed by the sea water, since its ends are attached to rests of the mooring line, see Figure 1. In order to apply Archimedes' force it is necessary to follow a derivation of Sparks [11], illustrated in Figure 2.

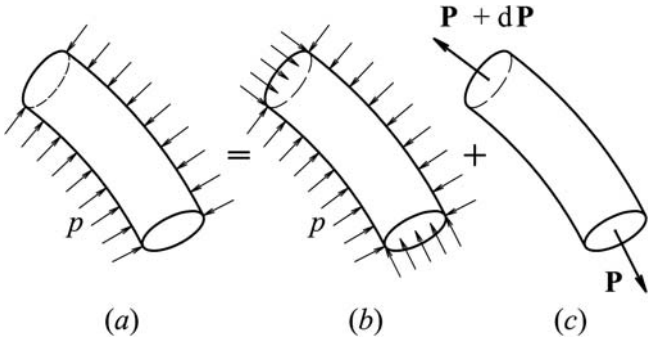

Figure 2 **Transformation of the hydrostatic pressure distribution**
Slika 2 **Transformacija rasporeda hidrostatskog tlaka**

The real distribution of the hydrostatic pressure acting on the segment (a) is replaced by a sum of the hydrostatic pressure of the completely immersed segment or distributed buoyancy (b) and outward-pointing forces at the segment's ends (c). Absolute value of the first outward-pointing force is given as

$$|\mathbf{P}| = pA, \tag{3}$$

where A is cross-section area of the mooring line. In the next step it is necessary to define equivalent loads and forces acting on the segment. Distributed buoyancy $\mathbf{q}_B$ is added to distributed load of the segment, see Figure 2 part (b)

$$\mathbf{q}_E = \mathbf{q}_B + \mathbf{q}, \tag{4}$$

where $\mathbf{q}_E$ is effective distributed load. Force $\mathbf{P}$ must be added to the internal force $\mathbf{F}$

$$\mathbf{F}_E = \mathbf{F} + \mathbf{P}, \tag{5}$$

where $\mathbf{F}_E$ represents cross-section effective force. According to (4) and (5) it is possible to define an equivalent segment of the mooring line, presented in Figure 3.

Force equilibrium on the equivalent segment of the mooring line leads to the motion equation

$$\frac{\mathrm{d}\mathbf{F}_E}{\mathrm{d}\tilde{s}} + \mathbf{q}_E = \tilde{m}\ddot{\mathbf{r}}, \tag{6}$$

where superposed dot denotes differentiation with respect to time. Moment equilibrium on the equivalent segment can be expressed as

$$\frac{\mathrm{d}\mathbf{r}}{\mathrm{d}\tilde{s}} \times \mathbf{F}_E = \mathbf{0}, \tag{7}$$

where × denotes vector product. The vector product from the right hand side of (6) with d**r**/d $\tilde{s}$ yields, after some manipulations of triple vector product [10]

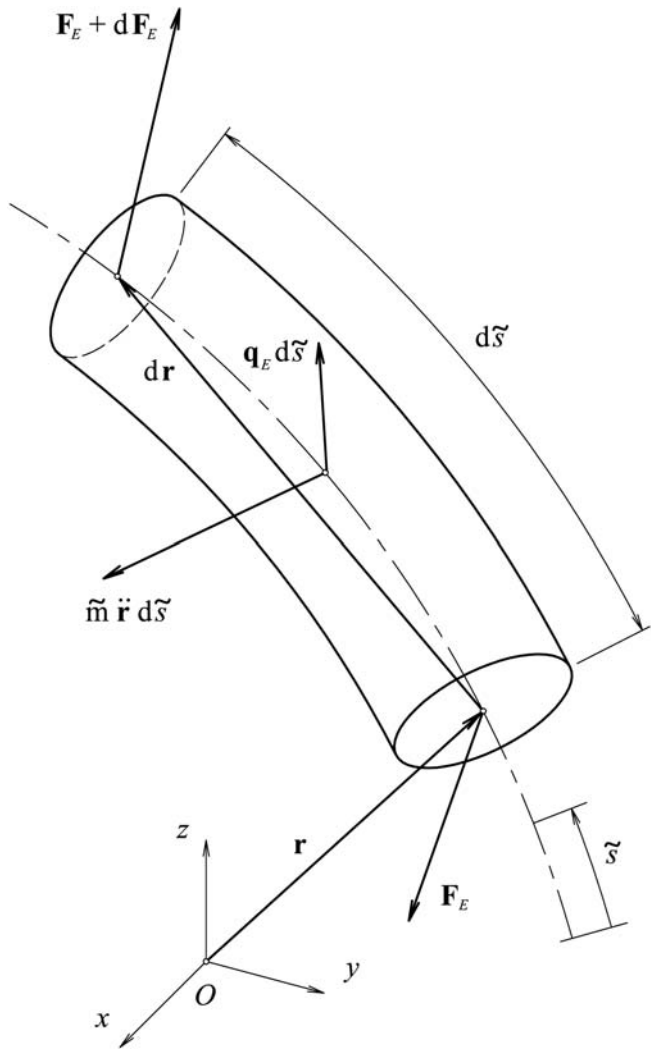

Figure 3 **Equivalent segment of the mooring line**
Slika 3 **Ekvivalentni diferencijalni element sidrene linije**

$$\left(\frac{\mathrm{d}\mathbf{r}}{\mathrm{d}\tilde{s}} \cdot \frac{\mathrm{d}\mathbf{r}}{\mathrm{d}\tilde{s}}\right)\mathbf{F}_E - \left(\frac{\mathrm{d}\mathbf{r}}{\mathrm{d}\tilde{s}} \cdot \mathbf{F}_E\right)\frac{\mathrm{d}\mathbf{r}}{\mathrm{d}\tilde{s}} = \mathbf{0}, \tag{8}$$

where · denotes scalar product. According to (1) and (2) d**r**/d $\tilde{s}$ is the unit tangent vector **u** of the space curve, so the following equation can be formed

$$\frac{\mathrm{d}\mathbf{r}}{\mathrm{d}\tilde{s}} \cdot \frac{\mathrm{d}\mathbf{r}}{\mathrm{d}\tilde{s}} = 1. \tag{9}$$

The term contained in the second parentheses of (8) represents scalar projection of $\mathbf{F}_E$ in the direction of the unit tangent vector **u**. Overview of Figure 4 leads to

$$T_E = \frac{\mathrm{d}\mathbf{r}}{\mathrm{d}\tilde{s}} \cdot \mathbf{F}_E. \tag{10}$$

Scalar variable T_E in the previous equation denotes effective tension force [11], [12]. Eq. (8) is simplified using (9) and (10)

$$\mathbf{F}_E = T_E \frac{\mathrm{d}\mathbf{r}}{\mathrm{d}\tilde{s}}. \tag{11}$$

Next, combining (6) and (11) leads to

$$\frac{\mathrm{d}}{\mathrm{d}\tilde{s}}\left(T_E \frac{\mathrm{d}\mathbf{r}}{\mathrm{d}\tilde{s}}\right) + \mathbf{q}_E = \tilde{m}\ddot{\mathbf{r}}. \tag{12}$$

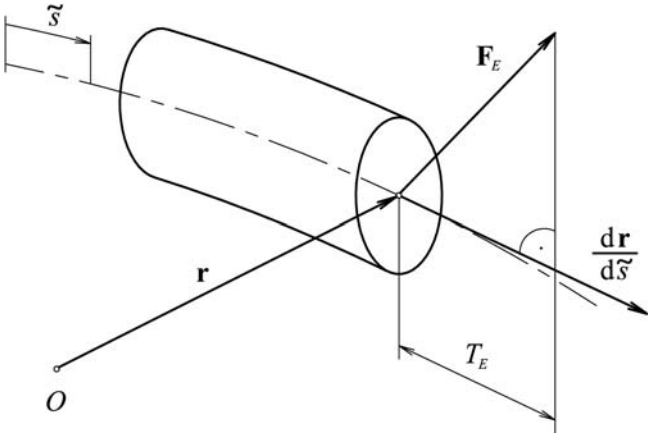

Figure 4 **Effective tension force**
Slika 4 **Efektivna vlačna sila**

Under applied internal and external forces the segment of the mooring line is extended to the length $\mathrm{d}\tilde{s}$. The elongation ε is defined, using a standard engineering definition

$$\varepsilon = \frac{\mathrm{d}\tilde{s} - \mathrm{d}s}{\mathrm{d}s}, \tag{13}$$

where ds is length of the non-extended segment. Relation between $\mathrm{d}\tilde{s}$ and ds now can be given as

$$\mathrm{d}\tilde{s} = (1+\varepsilon)\mathrm{d}s. \tag{14}$$

Upon substitution of (14) into (12), the final form of motion equation is obtained

$$\frac{\mathrm{d}}{\mathrm{d}s}\left(\frac{T_E}{1+\varepsilon}\frac{\mathrm{d}\mathbf{r}}{\mathrm{d}s}\right) + (1+\varepsilon)\mathbf{q}_E = (1+\varepsilon)\tilde{m}\ddot{\mathbf{r}}. \tag{15}$$

In (15) there are three unknown variables: $\mathbf{r}$, T_E and ε; therefore it is necessary to define additional two equations.

2.1.2 Axial elongation condition

The centreline of the deformed mooring line is described by the space curve. Eqs. (1) and (2) define the unit tangent vector $\mathbf{u}$ of the curve. Relationship between arc-length of the extended and the non-extended segment of the mooring line is given by (14). Based on these equations the axial elongation condition is formulated [13]

$$\frac{1}{(1+\varepsilon)^2}\frac{\mathrm{d}\mathbf{r}}{\mathrm{d}s}\cdot\frac{\mathrm{d}\mathbf{r}}{\mathrm{d}s} = 1. \tag{16}$$

This condition interconnects the deformed position and the elongation of the mooring line.

2.1.3 Effective tension-elongation relation

The elongation ε of the mooring line can be given in classical form [11], involving Young's modulus E and Poisson's ratio ν

$$\varepsilon = \frac{1}{E}\left[\sigma_A - \nu(\sigma_C + \sigma_R)\right], \tag{17}$$

where σ_A, σ_C and σ_R are the axial, the circumferential and the radial stress, respectively. Dividing the real tension force T_R in the mooring line by the cross-section area A gives the axial stress

$$\sigma_A = \frac{T_R}{A}. \tag{18}$$

Both the circumferential and the radial stress vary as a function of a radial distance from the mooring line axis, but their sum is constant. At any point on the cross-section sum of these stresses is defined by Lamé's formula

$$\sigma_C + \sigma_R = -2p, \tag{19}$$

where p is hydrostatic pressure of the surrounding sea water.

The effective tension force T_E is decomposed into two components, upon substitution of (5) in (10)

$$T_E = \frac{\mathrm{d}\mathbf{r}}{\mathrm{d}\tilde{s}}\cdot\mathbf{F} + \frac{\mathrm{d}\mathbf{r}}{\mathrm{d}\tilde{s}}\cdot\mathbf{P}. \tag{20}$$

The first component is scalar projection of the cross-area internal force $\mathbf{F}$ onto the unit tangent vector $\mathrm{u} = \mathrm{d}\mathbf{r}/\mathrm{d}\tilde{s}$. The obtained scalar variable is real tension force T_R and can be calculated analogous to (10)

$$T_R = \frac{\mathrm{d}\mathbf{r}}{\mathrm{d}\tilde{s}}\cdot\mathbf{F}. \tag{21}$$

Similar, the second component is simplified as

$$|\mathbf{P}| = \frac{\mathrm{d}\mathbf{r}}{\mathrm{d}\tilde{s}}\cdot\mathbf{P} \tag{22}$$

since vectors $\mathbf{P}$ and $\mathrm{d}\mathbf{r}/\mathrm{d}\tilde{s}$ are parallel, see Figure 2. Using (3), the second component is even more simplified

$$pA = \frac{\mathrm{d}\mathbf{r}}{\mathrm{d}\tilde{s}}\cdot\mathbf{P} \tag{23}$$

Upon substitution of (21) and (23) into (20), another equation is obtained that connects the real and the equivalent segment of the mooring line, see subsection: ***Motion equation***

$$T_E = T_R + pA\,. \tag{24}$$

Relationship between the real tension T_R and the effective tension T_E is defined in (24). Similar formula can be found in [12]. Next, the axial stress σ_A in (18) is given in the form suitable for further derivations using (24)

$$\sigma_A = \frac{T_E - pA}{A}. \tag{25}$$

Based on (17), (19) and (25) a new definition of the elongation ε is obtained

$$\varepsilon = \frac{1}{E}\left[\frac{T_E}{A} - (1-2\nu)p\right]. \tag{26}$$

For synthetic ropes Poisson's ratio is assumed to be [8]

$$\nu \approx 0.5. \tag{27}$$

The final form of effective tension-elongation relationship is defined by (26) and (28)

$$\varepsilon = \frac{T_E}{AE}. \tag{28}$$

2.1.4 Axial stiffness of polyester rope

The elongation of a polyester rope does not have linear relationship with its tension. A direct simulation of the polyester rope dynamics is extremely complicated. To simplify numerical simulation an empirical formulation is used to model axial stiffness *AE* of the polyester rope [9]

$$AE = RHOL\left(\alpha + \beta\frac{T_R}{B_S}\right)\cdot 10^6 \ \ [\mathrm{N}], \tag{29}$$

where B_S is minimum breaking strength, T_R is time dependant real tension, and *RHOL* is dry weight per unit length of the rope. Constants α and β depend on the type of polyester rope and they are obtained experimentally. The stiffness described by (29) is formulated in terms of the dynamics analysis but it is often used for static calculations. A similar definition of polyester Young's modulus can be found in [7].

2.1.5 Finite element for the static analysis

The effective distributed load $\mathbf{q}_E$ for the static analysis of the mooring line is formulated according to (4)

$$\mathbf{q}_E = \mathbf{q}_B + \mathbf{q}_G, \tag{30}$$

where $\mathbf{q}_G$ is distributed weight of dry mooring line. Distributed buoyancy $\mathbf{q}_B$ is given as

$$\mathbf{q}_B = -\rho\tilde{A}\mathbf{g}, \tag{31}$$

where ρ is density of the sea water, and $\mathbf{g}$ is gravitational acceleration. Similarly, $\mathbf{q}_G$ is expressed as

$$\mathbf{q}_G = \tilde{m}\mathbf{g}. \tag{32}$$

In the above equations, variables $\tilde{A}$ and $\tilde{m}$ are related to the extended case of the mooring line, so they depend on the elongation ε. Already in this paper, the Poisson's ratio of polyester rope is assumed to be 0.5, see (27). Therefore, the volume of any deformed segment is conserved [8]. The cross-section area $\tilde{A}$ and the distributed mass $\tilde{m}$ are formulated as

$$\tilde{A} = \frac{A}{1+\varepsilon} \tag{33}$$

$$\tilde{m} = \frac{m}{1+\varepsilon}, \tag{34}$$

where *A* and *m* are related to the non-extended case, so they are constant. Finally, by omitting inertial term in the motion equation (15) and combining with from (30) to (34), the static equation is defined as

$$\frac{\mathrm{d}}{\mathrm{d}s}\left(\frac{T_E}{1+\varepsilon}\frac{\mathrm{d}\mathbf{r}}{\mathrm{d}s}\right) + m\mathbf{g} - \rho A\mathbf{g} = \mathbf{0}. \tag{35}$$

The elongation ε formulated by (28) is included in the static equation (35) and the axial elongation condition (16) in inconvenient way for further derivations. Simplification is obtained by using Taylor series [10] for (35)

$$\frac{1}{1+\varepsilon} = 1 - \varepsilon + \varepsilon^2 + O(\varepsilon^3) \tag{36}$$

and for (16)

$$\frac{1}{(1+\varepsilon)^2} = 1 - 2\varepsilon + 3\varepsilon^2 + O(\varepsilon^3). \tag{37}$$

The final form of governing equations for the static analysis is composed of (16), (28) and (35) with simplifications according to (36), (37)

$$\frac{\mathrm{d}}{\mathrm{d}s}\left[\left(T_E - T_E\frac{T_E}{AE} + T_E\left(\frac{T_E}{AE}\right)^2\right)\frac{\mathrm{d}\mathbf{r}}{\mathrm{d}s}\right] + m\mathbf{g} - \rho A\mathbf{g} = \mathbf{0} \tag{38}$$

and

$$\left[1 - 2\frac{T_E}{AE} + 3\left(\frac{T_E}{AE}\right)^2\right]\frac{\mathrm{d}\mathbf{r}}{\mathrm{d}s}\cdot\frac{\mathrm{d}\mathbf{r}}{\mathrm{d}s} = 1. \tag{39}$$

It should be noted that (39) is intentionally defined in approximate form. By observing (16) and (28) an exact form of the axial elongation condition can be obtained, simply by multiplying (16) with $(1+\varepsilon)^2$. As it will be written below, this approximate form of eq. (39) provides a symmetric equation set for numerical calculations.

In (38) and (39) there are two unknown variables: effective tension T_E and the position vector of mooring line $\mathbf{r}$. This equation set is solved utilizing finite element method (FEM). The application of FEM starts from describing (38) and (39) in index notation

$$\left[\left(T_E - T_E\frac{T_E}{AE} + T_E\left(\frac{T_E}{AE}\right)^2\right)r_i'\right]' + m\mathbf{g}_i - \rho A\mathbf{g}_i = 0 \tag{40}$$

and

$$\left[1 - 2\frac{T_E}{AE} + 3\left(\frac{T_E}{AE}\right)^2\right]r_j'r_j' = 1, \tag{41}$$

with

$$i, j = 1, 2, 3 \tag{42}$$

where prime denotes differentiation with respect to *s*. Here unknown variables T_E and r_i are approximated as [14]

$$r_i(s) = A_l(s)\,U_{il} \tag{43}$$

$$T_E(s) = P_m(s)\,\lambda_m \tag{44}$$

with

$$m = 1, 2, 3; \quad l = 1, ..., 4 \tag{45}$$

where A_l and P_m are shape functions defined in the interval $0 \le s \le L$, where L is length of finite element, see Appendix A. Unknown coefficients U_{il} and λ_m can be expresed as

$$\begin{aligned} U_{i1} &= r_i(0); \quad U_{i2} = r_i'(0) \\ U_{i3} &= r_i(L); \quad U_{i4} = r_i'(L) \end{aligned} \tag{46}$$

and

$$\begin{aligned} \lambda_1 &= T_E(0) \\ \lambda_2 &= T_E(L/2). \\ \lambda_3 &= T_E(L) \end{aligned} \tag{47}$$

Galerkin method [15] combining with (43) and (44) is used for the finite element discretization of the static equation (40) as follows

$$\left(K^0_{nijkl} + \lambda_m K^1_{nmijkl} + \lambda_m\lambda_p K^2_{nmpijkl}\right)\lambda_n U_{jk} + F_{il} = 0, \tag{48}$$

with

$$K^0_{nijkl} = -\int_0^L P_n A_k' A_l' \delta_{ij}\,\mathrm{d}s \tag{49}$$

$$K^1_{nmijkl} = \int_0^L \frac{1}{AE} P_n P_m A_k' A_l' \delta_{ij}\,\mathrm{d}s \tag{50}$$

$$K^2_{nmpijkl} = -\int_0^L \frac{1}{(AE)^2} P_n P_m P_p A_k' A_l' \delta_{ij}\,\mathrm{d}s \tag{51}$$

$$F_{il} = F^C + \int_0^L m g_i\,\mathrm{d}s - \int_0^L (\rho A) g_i A_l\,\mathrm{d}s \tag{52}$$

and

$$n, p = 1, 2, 3; \; k = 1, ..., 4. \tag{53}$$

where δ_{ij} is Kronecker delta. Eq. (48) is the static equation of finite element, where F_{il} denotes total nodal forces that incorporate external nodal forces F^C_{il} as well as nodal forces from distributed dry weight and buoyancy of the mooring line. K^0_{nijkl} is geometric stiffness matrix of the non-extended mooring line. Additional stiffness matrices K^1_{nmijkl} and $K^2_{nmpijkl}$ can be considered as change coefficients of the geometric stiffness due to the elongation of the mooring line. To clarify, these additional matrices are direct consequence of the simplification used in the mooring line static (35). The simplification is carried out by Taylor series defined in (36). Obtained simplified form is shown in (40) using index notation. By close inspection of (40) and (48) the origin of each stiffness matrix can be determined. Thus, the geometric stiffness K^0_{nijkl} in (48) derives from $\left[T_E r_i'\right]'$ in (40). In the same way, additional stiffness matrices K^1_{nmijkl} and $K^2_{nmpijkl}$ are derived from $\left[T_E\left(T_E/AE\right)r_i'\right]'$ and $\left[T_E\left(T_E/AE\right)^2 r_i'\right]'$ respectively. Further, heaving in mind that the term T_E/AE is the mooring line elongation ε according to (28), K^1_{nmijkl} can be considered as linear and $K^2_{nmpijkl}$ quadratic change coefficient of the geometric stiffness.

Axial elongation condition (41) is also discretized using Galerkin's method [15] and combining with (43) and (44) as follows

$$\left(B^0_{mkl} + \lambda_n B^1_{nmkl} + \lambda_n\lambda_p B^2_{nmpkl}\right)U_{jl}U_{jk} - C_m = 0, \tag{54}$$

with

$$B^0_{mkl} = \int_0^L P_m A_k' A_l'\,\mathrm{d}s \tag{55}$$

$$B^1_{nmkl} = -\int_0^L \frac{2}{AE} P_n P_m A_k' A_l'\,\mathrm{d}s \tag{56}$$

$$B^2_{nmpkl} = \int_0^L \frac{3}{(AE)^2} P_n P_m P_p A_k' A_l'\,\mathrm{d}s \tag{57}$$

$$C_m = \int_0^L P_m\,\mathrm{d}s. \tag{58}$$

Finite element static equation (48) and discretized axial elongation condition (54) are highly nonlinear. Therefore, this equation system is solved using the Newton-Rapson iterative method [10] as follows

$$\begin{bmatrix} J^{11(k)}_{ijkl} & J^{12(k)}_{nil} \\ J^{21(k)}_{mjk} & J^{22(k)}_{mn} \end{bmatrix}\begin{Bmatrix} \Delta U_{jk} \\ \Delta\lambda_n \end{Bmatrix} = -\begin{Bmatrix} R^{1(k)}_{il} \\ R^{2(k)}_{m} \end{Bmatrix}, \tag{59}$$

with

$$J^{11(k)}_{ijkl} = \left(K^0_{nijkl} + \lambda_m K^1_{nmijkl} + \lambda_m\lambda_p K^2_{nmpijkl}\right)^{(k)}\lambda_n^{(k)} \tag{60}$$

$$J^{12(k)}_{nil} = \left(K^0_{nijkl} + 2\lambda_m K^1_{nmijkl} + 3\lambda_m\lambda_p K^2_{nmpijkl}\right)^{(k)} U^{(k)}_{jk} \tag{61}$$

$$J^{21(k)}_{mjk} = -\left(B^0_{mkl} + \lambda_n B^1_{nmkl} + \lambda_n\lambda_p B^2_{nmpkl}\right)^{(k)} U^{(k)}_{jl} \tag{62}$$

$$J^{22(k)}_{mn} = -\frac{1}{2}\left(B^1_{nmkl} + 2\lambda_p B^2_{nmpkl}\right)^{(k)} U^{(k)}_{jl} U^{(k)}_{jk} \tag{63}$$

$$R^{1(k)}_{il} = J^{11(k)}_{ijkl} U^{(k)}_{jk} + F^{(k)}_{il} \tag{64}$$

$$R^{2(k)}_{m} = \frac{1}{2}\left(J^{21(k)}_{mjk} U^{(k)}_{jk} + C_m\right). \tag{65}$$

In (59) J^{11}_{ijkl}, J^{12}_{nil}, J^{21}_{mjk}, J^{22}_{mn} and denote parts of a Jacobian matrix while R^1_{il} and R^2_m compose a residual vector. Label (k) in superscripts denotes number of iteration. Simplified form of eq. (59) for a single finite element is given as

$$\left[J\right]^{(k)}\left\{\Delta y\right\} = -\left\{R\right\}^{(k)}, \tag{66}$$

where

$$\left\{y\right\} = \left\{U_{11}\,U_{12}\,U_{21}\,U_{22}\,U_{31}\,U_{32}\,\lambda_1\,\lambda_2\,U_{13}\,U_{14}\,U_{23}\,U_{24}\,U_{33}\,U_{34}\,\lambda_3\right\}^T \tag{67}$$

$$\{R\} = \left\{ R_{11}^1\ R_{12}^1\ R_{21}^1\ R_{22}^1\ R_{31}^1\ R_{32}^1\ R_1^2\ R_2^2\ R_{13}^1\ R_{14}^1\ R_{23}^1\ R_{24}^1\ R_{33}^1\ R_{34}^1\ R_3^2 \right\}^T. \quad (68)$$

Calculations are carried out iteratively according to the following algorithm

$$\{\Delta Y\} = \left[K^{-1}\right]^{(k)} \{F\}^{(k)} \quad (69)$$

$$\{Y\}^{(k+1)} = \{Y\}^{(k)} + \{\Delta Y\}, \quad (70)$$

where $\{Y\}$ is global "nodal displacement" vector, $[K]$ global "stiffness" matrix and $\{F\}$ is global "nodal force" vector.

By detailed inspection of (59) it can be found that formulation of the Jacobian matrix is symmetrical. As it is known, the Jacobian matrix in most causes is not symmetric when a nonlinear equation system is considered. In this study special effort is invested to achieve this symmetrical form. The symmetry is mainly realized by selecting appropriate form of the axial elongation condition (16). As already written, by Taylor series in (37) and (28) an approximate form of axial elongation condition is given in (39). This form provided a requested basis for the symmetry. Furthermore, during formulation of the Newton-Rapson procedure (59), discretized axial elongation condition (54) is multiplied by -1/2 to achieve the complete symmetry. This symmetric form of the Jacobian matrix enables easier numerical implementation utilizing classical FEM codes.

2.1.6 Finite element for the dynamic analysis

Distributed hydrodynamic load $\mathbf{q}_H$ on the mooring line is derived utilizing Morison equation [14] as follows

$$\mathbf{q}_H = -C_A \rho A \ddot{\mathbf{r}}^n + C_M \rho A \dot{\mathbf{v}}^n + \frac{1}{2} C_D \rho D \left|\mathbf{v}^n - \mathbf{r}^n\right| \left(\mathbf{v}^n - \mathbf{r}^n\right) \quad (71)$$

with

$$\begin{aligned} \ddot{\mathbf{r}}^n &= \ddot{\mathbf{r}} - \left(\ddot{\mathbf{r}} \cdot \frac{\mathrm{d}\mathbf{r}}{\mathrm{d}s}\right) \frac{\mathrm{d}\mathbf{r}}{\mathrm{d}s} \\ \dot{\mathbf{r}}^n &= \dot{\mathbf{r}} - \left(\dot{\mathbf{r}} \cdot \frac{\mathrm{d}\mathbf{r}}{\mathrm{d}s}\right) \frac{\mathrm{d}\mathbf{r}}{\mathrm{d}s} \\ \dot{\mathbf{v}}^n &= \dot{\mathbf{v}} - \left(\dot{\mathbf{v}} \cdot \frac{\mathrm{d}\mathbf{r}}{\mathrm{d}s}\right) \frac{\mathrm{d}\mathbf{r}}{\mathrm{d}s} \\ \mathbf{v}^n &= \mathbf{v} - \left(\mathbf{v} \cdot \frac{\mathrm{d}\mathbf{r}}{\mathrm{d}s}\right) \frac{\mathrm{d}\mathbf{r}}{\mathrm{d}s} \end{aligned} \quad (72)$$

where $|\quad|$ denotes the length of a vector; A and D are cross-section area and diameter of the non-extended mooring line respectively; C_A, C_M and C_D are added mass, inertial and drag coefficients. In (72), $\ddot{\mathbf{r}}^n$ is a component of the mooring line acceleration normal to the mooring line, see Figure 5. Analogously, $\dot{\mathbf{r}}^n$ is the normal component of the mooring line velocity. Motion of the surrounding sea water is considered through normal components of water particle acceleration $\dot{\mathbf{v}}^n$ and velocity $\mathbf{v}^n$. In the next step, hydrodynamic load needs to be considered within the motion equation (15). Therefore, the effective distributed load $\mathbf{q}_E$ for dynamic analysis is formulated according to (4) and (30)

$$\mathbf{q}_E = \mathbf{q}_B + \mathbf{q}_G + \mathbf{q}_H. \quad (73)$$

The final form of motion equation is derived using (15), (31), (32), (33), (34) and (73) as follows

$$\frac{\mathrm{d}}{\mathrm{d}s}\left(\frac{T_E}{1+\varepsilon}\frac{\mathrm{d}\mathbf{r}}{\mathrm{d}s}\right) + m\mathbf{g} - \rho A\mathbf{g} + \mathbf{q}_H = m\ddot{\mathbf{r}}. \quad (74)$$

It should be noted that in the previous chapter the formulation of the distributed buoyancy $\mathbf{q}_B$ is based on the cross-section area $\tilde{A}$ of the extended mooring line, see (31). In (33), the relation of the cross-section area for extended and non-extended state is formulated based on the elongation ε. For sake of simplicity, the elongation ε is not considered in the derivation of distributed hydrodynamic load in (71), so the cross-section area A as well as the diameter D are assumed to be constant. With same intention, the elongation is neglected in the formulation of acceleration and velocity normal components in (72), where the unit tangent vector $\mathrm{d}\mathbf{r}/\mathrm{d}\tilde{s}$ of the extended mooring line is replaced by $\mathrm{d}\mathbf{r}/\mathrm{d}s$, see (1) and (14). The elongation is also neglected in the derivation of motion equation (74), so that the term $(1 + \varepsilon)$ that should multiply $\mathbf{q}_H$ is dropped, see (15) and (73).

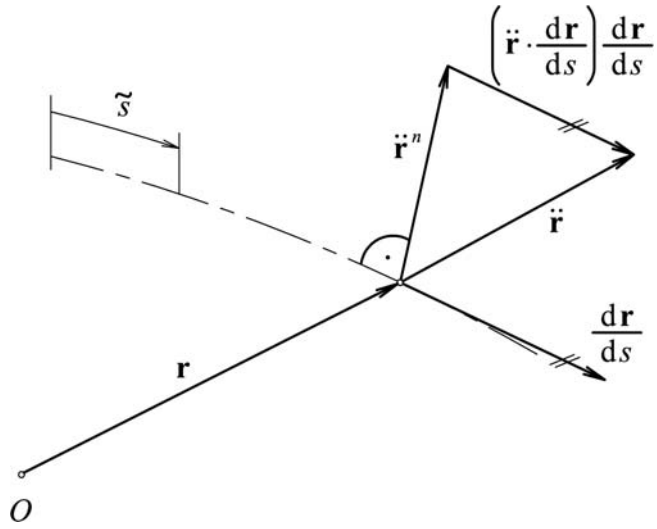

Figure 5 **Normal component of the mooring line acceleration**
Slika 5 **Normalna komponenta ubrzanja sidrene linije**

The axial elongation condition given by (16) must be fulfilled during dynamic analysis. To obtain symmetric equation set for numeric calculation an approximate form of the condition is chosen as follows

$$\frac{1}{1+\varepsilon}\left(\frac{\mathrm{d}\mathbf{r}}{\mathrm{d}s} \cdot \frac{\mathrm{d}\mathbf{r}}{\mathrm{d}s}\right) - 1 - \varepsilon = 0. \quad (75)$$

The final form of governing equations for dynamic analysis is composed of (28), (74) and (75) with simplification according to (36), given in index notation

$$\left[\left(T_E - T_E\frac{T_E}{AE} + T_E\left(\frac{T_E}{AE}\right)^2\right) r_i'\right]' + mg_i - \rho A g_i + q_i^H = m\ddot{r}_i \quad (76)$$

and

$$\left[1-\frac{T_E}{AE}+\left(\frac{T_E}{AE}\right)^2\right]r_j'\,r_j'-1-\frac{T_E}{AE}=0. \tag{77}$$

Note that in the above equations there is new label q_i^H for the hydrodynamic load to avoid confusion when using index notation. Unknown variables T_E and r_i are approximated in the same way as for static calculations by (43) and (44), in this case here unknown coefficients U_{il} and λ_m are time dependent.

Finite element discretization of the motion equation (76) is based on Galerkin's method [15] as follows

$$\begin{aligned}&\left(M_{ijkl}+M_{ijkl}^A\right)\ddot{U}_{jk}+\\&+\left(K_{nijkl}^0+\lambda_m K_{nmijkl}^1+\lambda_m\lambda_p K_{nmpijkl}^2\right)\lambda_n U_{jk}+F_{il}+F_{il}^H=0,\end{aligned} \tag{78}$$

with

$$M_{ijkl}=-\int_0^L mA_lA_k\delta_{ij}\,\mathrm{d}s \tag{79}$$

$$M_{ijkl}^A=-\int_0^L\left(C_A\,\rho A\right)A_l\,e_{ifg}\,A_v'\,e_{gjh}\,A_k\,A_z'U_{fv}U_{hz}\,\mathrm{d}s \tag{80}$$

$$\begin{aligned}F_{il}^H=&\int_0^L\left(C_M\,\rho A\right)A_l\,e_{ifg}\,A_v'\,e_{gjh}\,A_z'\dot{v}_j\,U_{fv}U_{hz}\,\mathrm{d}s+\\&+\int_0^L\left(\frac{1}{2}C_D\,\rho A\right)\sqrt{\left[e_{abc}\left(v_b-A_r\dot{U}_{br}\right)A_s'U_{cs}\right]\left[e_{ade}\left(v_d-A_l\dot{U}_{dt}\right)A_u'U_{eu}\right]}\cdot\\&\cdot\left[A_l\,e_{ifg}\,A_v'\,e_{gjh}\left(v_j-A_k\dot{U}_{jk}\right)A_z'\,U_{fv}U_{hz}\right]\mathrm{d}s\end{aligned} \tag{81}$$

and

$$a,b,c,d,e,f,g,h=1,2,3;\quad r,t,u,v,z=1,...,4. \tag{82}$$

where e_{ijk} is Levi-Civita symbol. Eq. (78) is the dynamic equation of finite element, where M_{ijkl} denotes mass matrix due to own mass; M_{ijkl}^A is added mass matrix and F_{il}^H is nodal force vector due to hydrodynamic load. Stiffness matrices K_{nijkl}^0, K_{nmijkl}^1 and $K_{nmpijkl}^2$ as well as nodal force vector F_{il} are the same as for the static case, see (48). The (78) is a second order differential equation. The order of this equation is derated using the first derivate of displacements. As a result, two first order differential equations are obtained, as follows

$$\hat{M}_{ijkl}\dot{V}_{jk}=-\hat{K}_{nijkl}\lambda_n U_{jk}-\hat{F}_{il} \tag{83}$$

$$\dot{U}_{jk}=V_{jk} \tag{84}$$

with substitutions

$$\hat{M}_{ijkl}=M_{ijkl}+M_{ijkl}^A \tag{85}$$

$$\hat{K}_{nijkl}=K_{nijkl}^0+\lambda_m K_{nmijkl}^1+\lambda_m\lambda_p K_{nmpijkl}^2 \tag{86}$$

$$\hat{F}_{il}=F_{il}+F_{il}^H, \tag{87}$$

where V_{jk} is nodal velocity vector. For the sake of simplicity, time integration is based on trapezoidal integration [10], with sequential formulas

$$V_{jk}^{(n+1)}=\frac{2}{\Delta t}\left(U_{jk}^{(n+1)}-U_{jk}^{(n)}\right)-V_{jk}^{(n)} \tag{88}$$

$$\dot{V}_{jk}^{(n+1)}=\frac{4}{\Delta t^2}\left(U_{jk}^{(n+1)}-U_{jk}^{(n)}\right)-\frac{4}{\Delta t}V_{jk}^{(n)}-\dot{V}_{jk}^{(n)}, \tag{89}$$

where Δt is time step size and n in superscripts denotes time step number. To achieve time integration of dynamic equation (78) it is necessary to combine (83) with the above formulas

$$\begin{aligned}&\hat{M}_{ijkl}^{(n+1)}\left[\frac{4}{\Delta t^2}\left(U_{jk}^{(n+1)}-U_{jk}^{(n)}\right)-\frac{4}{\Delta t}V_{jk}^{(n+1)}-\dot{V}_{jk}^{(n)}\right]=\\&=-\hat{K}_{nijkl}^{2(n+1)}\lambda_n^{(n+1)}U_{jk}^{(n+1)}-\hat{F}_{il}^{(n+1)}.\end{aligned} \tag{90}$$

Discretization of the axial extension condition (77) is also achieved using Galerkin's method and combining with (43) and (44), as follows:

$$(\hat{B}_{mkl}^0+\lambda_n\hat{B}_{nmkl}^1+\lambda_n\lambda_p\hat{B}_{nmpkl}^2)U_{jl}U_{jk}+\hat{C}_{nm}\lambda_n-C_m=0 \tag{91}$$

with

$$\hat{B}_{mkl}^0=\int_0^L P_mA_k'A_l'\,\mathrm{d}s \tag{92}$$

$$\hat{B}_{nmkl}^1=-\int_0^L\frac{1}{AE}P_nP_mA_k'A_l'\,\mathrm{d}s \tag{93}$$

$$\hat{B}_{nmpkl}^2=\int_0^L\frac{1}{(AE)^2}P_nP_mP_pA_k'A_l'\,\mathrm{d}s \tag{94}$$

$$\hat{C}_{nm}=-\int_0^L\frac{1}{AE}P_nP_m\,\mathrm{d}s. \tag{95}$$

Vector C_m is the same as for eq. (54).

Finite element dynamic equations with implemented time integration given by eq. (90) and discretizied axial elongation condition (91) are highly nonlinear. Therefore, the Newton-Rapson iterative method [10] is used to solve this equation set, as follows

$$\begin{bmatrix}\hat{J}_{ijkl}^{11(n+1,k)} & \hat{J}_{nil}^{12(n+1,k)}\\ \hat{J}_{mjk}^{21(n+1,k)} & \hat{J}_{mn}^{22(n+1,k)}\end{bmatrix}\begin{Bmatrix}\Delta U_{jk}\\ \Delta\lambda_n\end{Bmatrix}=-\begin{Bmatrix}\hat{R}_{il}^{1(n+1,k)}\\ \hat{R}_m^{2(n+1,k)}\end{Bmatrix}, \tag{96}$$

with

$$\hat{J}_{ijkl}^{11(n+1,k)}=\frac{4}{\Delta t^2}\hat{M}_{ijkl}^{(n+1,k)}+\hat{K}_{nijkl}^{(n+1,k)}\lambda_n \tag{97}$$

$$\hat{J}_{nil}^{12(n+1,k)}=\hat{K}_{nijkl}^{(n+1,k)}U_{jk}^{(n+1,k)} \tag{98}$$

$$\hat{J}_{mjk}^{21(n+1,k)}=-\left(\hat{B}_{mkl}^0+\lambda_n\hat{B}_{nmkl}^1+\lambda_n\lambda_p\hat{B}_{nmpkl}^2\right)^{(n+1,k)}U_{jl}^{(n+1,k)} \tag{99}$$

$$\hat{J}_{mn}^{22(n+1,k)}=-\frac{1}{2}\hat{C}_{mn}-\frac{1}{2}\left(\hat{B}_{nmkl}^1+2\lambda_p\hat{B}_{nmpkl}^2\right)^{(n+1,k)}U_{jl}^{(n+1,k)}U_{jk}^{(n+1,k)} \tag{100}$$

$$\begin{aligned}\hat{R}_{il}^{1(n+1,k)}=&\left(\frac{4}{\Delta t^2}\hat{M}_{ijkl}^{(n+1,k)}+\hat{K}_{nijkl}^{(n+1,k)}\lambda_n\right)U_{jk}^{(n+1,k)}+\hat{F}_{il}^{(n+1,k)}+\\&+\hat{M}_{ijkl}^{(n+1,k)}\left(-\frac{4}{\Delta t^2}U_{jk}^{(n)}-\frac{4}{\Delta t}V_{jk}^{(n)}-\dot{V}_{jk}^{(n)}\right)\end{aligned} \tag{101}$$

$$\hat{R}_m^{2(n+1,k)} = -\frac{1}{2}\left[\begin{matrix}\left(\hat{B}^0_{mkl} + \lambda_n \hat{B}^1_{nmkl} + \lambda_n \lambda_p \hat{B}^2_{nmpkl}\right)^{(n+1,k)} \\ U^{(n+1,k)}_{jl} U^{(n+1,k)}_{jk} + \hat{C}_{nm} \lambda_n^{(n+1,k)} - C_m\end{matrix}\right] \quad (102)$$

where k in superscripts denotes iteration number within a time step. In (96) $\hat{J}^{11}_{ijkl}, \hat{J}^{12}_{nil}, \hat{J}^{21}_{mjk}$ and $\hat{J}^{22}_{mn}$ compose a Jacobian matrix while $\hat{R}^1_{il}$ and $\hat{R}^2_m$ are parts of a residual vector. Simplified form of (96) for a single finite element is given as

$$\left[\hat{J}\right]^{(n+1,k)}\{\Delta y\} = -\left\{\hat{R}\right\}^{(n+1,k)}. \quad (103)$$

Algorithm for iterative calculations has the form

$$\{y\}^{(n+1,\,k+1)} = \begin{cases}\{y\}^{(n)} + \{\Delta y\} & \text{for } 1^{\text{st}} \text{ iteration} \\ \{y\}^{(n+1,k)} + \{\Delta y\} & \text{for other iterations}\end{cases}. \quad (104)$$

Detailed inspection of (96) reveals symmetric form of the Jacobian matrix. The symmetry is mostly achieved by selecting appropriate form of the axial elongation condition in (75). Also, during derivation of the Newton-Rapson method given by (96), discretized axial elongation condition (91) is multiplied by -1/2 to fully realize the symmetry.

2.2 Time domain hydrodynamics of a floating body

Hydrodynamics of a floating body in the time domain is defined by Cummins [16], in the following form

$$\left(\left[M^m\right]+\left[A^\infty\right]\right)\left\{\ddot{\xi}(t)\right\} + \int_0^t \left[K(t-\tau)\right]\left\{\dot{\xi}(\tau)\right\}\mathrm{d}\tau + \\ +\left[C^h\right]\{\xi(t)\} = \{F(t)\}, \quad (105)$$

where

- $\{\xi(t)\}$ – displacement vector of a floating body dependant on time
- $\left[M^m\right]$ – mass matrix due to own mass of a floating body
- $\left[A^\infty\right]$ – added mass independent of frequency (or added mass for the time domain)
- $\left[C^h\right]$ – hydrostatic stiffness matrix
- $\left[K(t)\right]$ – matrix of impulse response function (memory function)
- $\{F(t)\}$ – excitation force vector,

It is shown in [16] that the impulse response function can be calculated from frequency dependant damping coefficients $[B(\omega)]$

$$\left[K(t)\right] = \frac{2}{\pi}\int_0^\infty \left[B(\omega)\right]\cos(\omega t)\,\mathrm{d}\omega. \quad (106)$$

Added mass in (105) is defined by Ogilvie [17] as follows

$$\left[A^\infty\right] = \left[A(\omega_{AC})\right] + \frac{1}{\omega_{AC}}\int_0^\infty \left[K(t)\right]\sin(\omega_{AC} t)\,\mathrm{d}t, \quad (107)$$

where

- $[A(\omega)]$ – frequency dependant added mass
- ω_{AC} – arbitrary chosen frequency

Considering a moored floating object, excitation force vector $\{F(t)\}$ is calculated as

$$\{F(t)\} = \left\{F_W^{(1)}(t)\right\} + \left\{F_W^{(2)}(t)\right\} + \left\{F_{WN}(t)\right\} + \left\{F_{CR}(t)\right\} + \left\{F_{VD}(t)\right\}, \quad (108)$$

where

- $\left\{F_W^{(1)}(t)\right\}$ – wave loads of the first order on a floating object (in the time domain)
- $\left\{F_W^{(2)}(t)\right\}$ – wave loads of the second order
- $\left\{F_{WN}(t)\right\}$ – wind loads
- $\left\{F_{CR}(t)\right\}$ – sea current loads
- $\left\{F_{VD}(t)\right\}$ – viscous drag loads.

Calculation procedures of the above listed loads are shown in Appendix B.

2.3 Coupled model

For complete description of the moored object response it is necessary to develop a coupled model. In this study, the coupling is achieved on the floating object's connection points with the mooring lines. At each connection point, two conditions must be fulfilled.

The first condition requires that the upper end of the mooring line has the same displacement in time as the connection point on the floating object. This condition is usually called a displacement compatibility and in this case is formulated using Figure 6, where

- $0xyz$ – fixed Cartesian coordinate system
- $\bar{G}\bar{x}\bar{y}\bar{z}$ – coordinate system of the floating object
- $G, \bar{G}$ – initial and current centre of gravity of the floating object, respectively
- $P, \bar{P}$ – initial and current connection point on the floating object, respectively
- $\mathbf{r}_G$ – position vector of G

Figure 6 **The displacement compatibility of $\bar{P}$**
Slika 6 **Kompatibilnost pomaka točke $\bar{P}$**

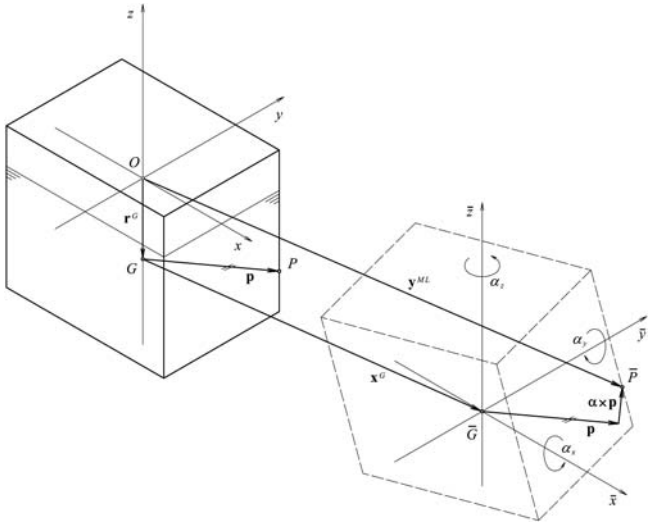

$\mathbf{x}^G$, $\boldsymbol{\alpha}$ – translational and angular displacement vector of the floating object, respectively
$\mathbf{p}$ – position vector of P in regard to G
$\mathbf{y}^{ML}$ – position vector of the upper end of the mooring line.

According to Figure 6, the displacement compatibility is formulated for $\overline{P}$ as follows

$$\mathbf{y}^{ML} = \mathbf{r}^G + \mathbf{x}^G + \mathbf{p} + \alpha \times \mathbf{p}. \tag{109}$$

The second condition is based on the equilibrium of forces at the connection point defined as

$$\mathbf{F}^{FC} + \mathbf{F}^{MC} = \mathbf{0}, \tag{110}$$

where
$\mathbf{F}^{FC}$ – force on the floating object due to the mooring line
$\mathbf{F}^{MC}$ – force on the mooring line due to the floating object.

To carry out calculation of the coupled model, the force $\mathbf{F}^{MC}$ must be taken into account when defining the global force vector of the corresponding mooring line, see (69). Similar, the force $\mathbf{F}^{FC}$ should be considered when defining governing equation (105) of the floating object. In this case, the moment regarding the centre of gravity caused by $\mathbf{F}^{FC}$ should also be considered.

3 Case study I - single mooring line

This case study is based on observation of Tahar & Kim [9] who have considered a single polyester mooring line. The mooring line is placed vertically, and it is used for a buoy, see Figure 7.

Figure 7 **Single mooring line**
Slika 7 **Jednostruka sidrena linija**

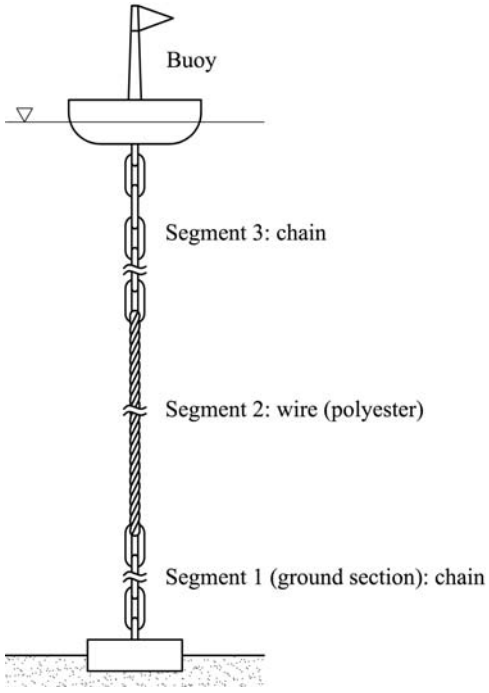

It is assumed that the buoy is floating at calm free surface of the sea. Hydrodynamic loads as well as environmental loads are not taken into account. Properties of the mooring line are given in Table 1.

Table 1 **Properties of the single mooring line**
Tablica 1 **Značajke sidrene linije**

Designation	Quantity	Unit
Pretension	412.8	kN
Length	914.4	m
Segment 1 (ground section): chain		
Length	12.19	m
Diameter	70	mm
Distributed mass	30.2	kg/m
Wet weight	258	N/m
Stiffness *AE*	$1.08 \cdot 10^5$	kN
Minimum breaking load (*MBL*)	$11.8 \cdot 10^3$	kN
Segment 2: wire (polyester)		
Length	856.49	m
Diameter	85	mm
Distributed mass - *RHOL*	5.06	kg/m
Wet weight	12.3	N/m
Linearized stiffness	$2.429 \cdot 10^4$	kN
Stiffness parameters:		
α	2.5	
β	2.0	
Minimum breaking load (*MBL*)	$1.97 \cdot 10^3$	kN
Segment 3: chain		
Length	45.72	m
Other parameters are the same as for the segment 1.		

Static case

Initial state is characterized by a pretension force and associated elongation of the mooring line. This force is applied at the

Figure 8 **The relation vertical force-elongation of single mooring line with linearized material properties**
Slika 8 **Odnos vertikalne sile i istezanja sidrene linije s linearizirani značajkama materijala**

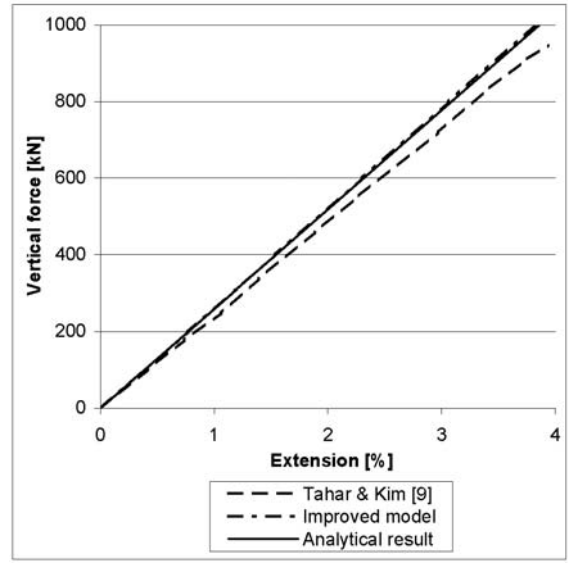

upper end of the mooring line. At the same position additional vertical force is applied with the maximum value of 10^3 kN. Material of the mooring line is assumed to be linear. The relationship between the vertical force and the elongation obtained by the improved model developed in this paper is shown in Figure 8. Within this model 22 finite elements were used. Out of these elements one element is used for each chain segment. For this case it is possible to obtain an analytical solution, see Appendix C. The analytical result is also shown in Figure 8 for comparison, alongside with result from Tahar & Kim [9].

Next, the nonlinear properties of the polyester rope are considered, see (29). The results of these calculations are presented in Fig. 9.

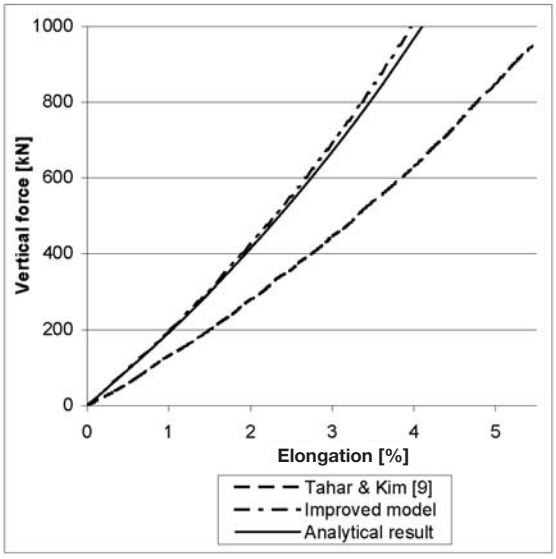

Figure 9 **The relation vertical force-elongation of single mooring line with nonlinear material properties**
Slika 9 **Odnos vertikalne sile i istezanja sidrene linije s nelinearnim značajkama materijala**

4 Case study II - spar platform

Input data for this case study are found in Arcandra [14]. A spar platform moored by polyester ropes is considered. The sea depth is 1 830 m. Characteristics of the platform are given in Table 2. A taut mooring system consisting of four identical mooring lines is used, see Figure 10. Properties of the mooring lines are shown in Table 3. Wind, wave and sea current loads are coming from different directions, see Table 4.

Table 2 **Characteristics of the spar platform**
Tablica 2 **Značajke spar platforme**

Designation	Quantity	Unit
Length	214.88	m
Draught	198.12	m
KB	164.59	m
KG	129.84	m
Displacement	220 740	t
Pitch radius of gyration in air	67.36	m
Yaw radius of gyration in air	8.69	m
Drag force coefficient	1.15	
Wind force coefficient	2 671.59	N/(m/s)^2

Table 3 **Properties of mooring lines for the spar platform**
Tablica 3 **Značajke sidrenih linija spar platforme**

Designation	Quantity	Unit
Pretension	2357	kN
Length	2590.8	m
Fairlead location above base line	91.44	m
Segment 1 (ground section): chain		
Length	121.92	m
Diameter	245	mm
Distributed mass	287.8	kg/m
Wet weight	2 485	N/m
Stiffness *AE*	$1.03 \cdot 10^6$	kN
Minimum breaking load (*MBL*)	$11.8 \cdot 10^3$	kN
Distributed added mass	37.4	kg/m
Drag force coefficient	2.45	
Segment 2: wire (polyester)		
Length	2 377.44	m
Diameter	210	mm
Distributed mass - *RHOL*	36.52	kg/m
Wet weight	75.5	N/m
Linearized stiffness *AE*	$3.18 \cdot 10^5$	kN
Minimum breaking load (*MBL*)	$12.79 \cdot 10^3$	kN
Distributed added mass	28.8	kg/m
Drag force coefficient	1.2	
Segment 3: chain		
Length	91.44	m
Other parameters are the same as for the segment 1.		

Table 4 **Environmental conditions for the spar platform**
Tablica 4 **Opterećenje okoliša na spar platformu**

Designation		Quantity	Unit
Waves			
H_s:		6.19	m
T_p:		14	s
Wave spectrum		JONSWAP ($\gamma = 2.5$)	
Wave direction		180	degree
Wind			
Wind speed (1 h):		16.28	m/s @ 10 m
Wind spectrum		API RP 2A-WSD	
Wind direction		210	degree
Sea current			
Profile:			
depth	: 0 m	0.0668	m/s
	: 60.96 m	0.0668	m/s
	: 91.44 m	0.0014	m/s
	seabed	0.0014	m/s
Current direction		150	degree

Dynamic case

Each mooring line is modelled by 7 finite elements, and one of them is used for each chain segment. Length of the time step is 0.2 s, see (83) to (90). Within each time step 3 iterations are carried out, see (96) to (104). Hydrodynamic calculations are done using HYDROSTAR [18]. The obtained numerical results are shown in the following figures.

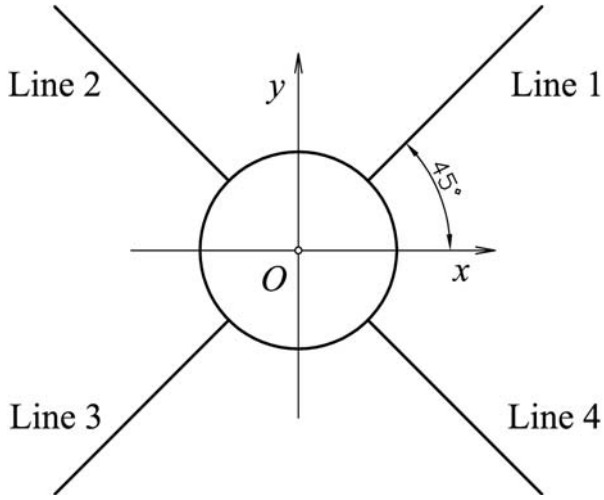

Figure 10 **Arrangement of mooring lines of the spar platform**
Slika 10 **Raspored sidrenih linija spar platforme**

Figure 11 **Displacements of the spar platform**
Slika 11 **Pomaci spar platforme**

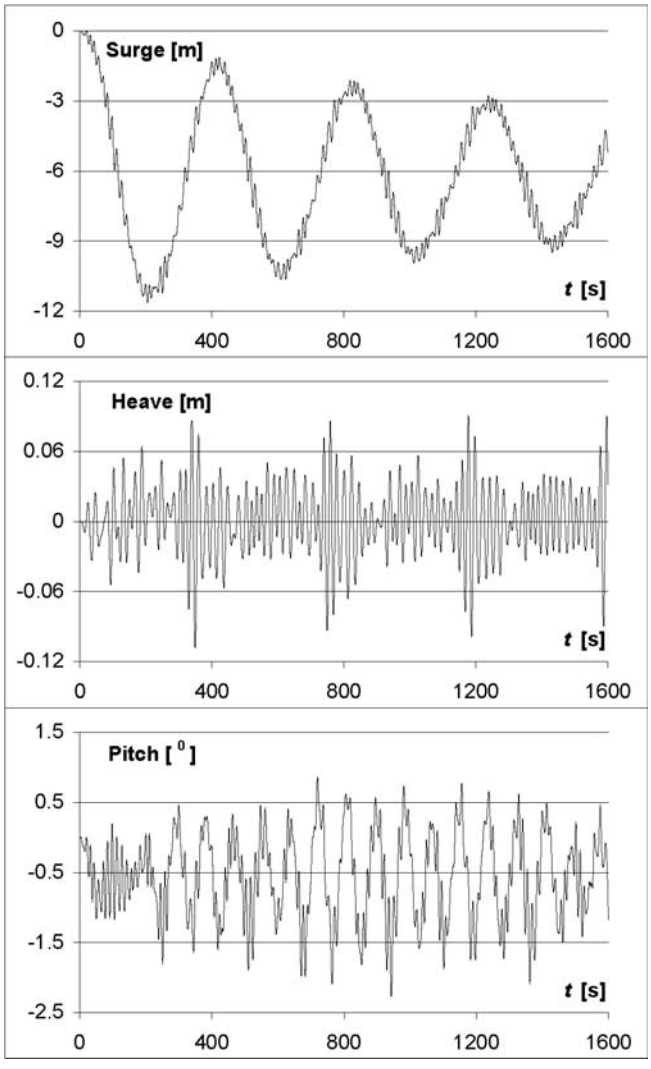

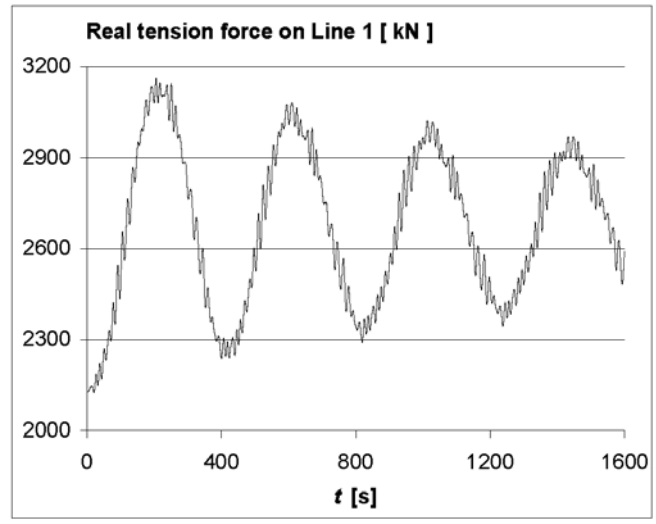

Figure 12 **Real tension force on the upper end of the first mooring line (of the spar platform)**
Slika 12 **Realna vlačna sila na gornjem kraju prve sidrene linije (spar platforme)**

5 Conclusion

In this study, high elongation of polyester mooring lines is considered within a stiffness model in a new, improved way. The nonlinear tension-elongation relation of a polyester rope is a part of the improved stiffness model. Development of the model is done considering the coupled dynamic analysis of a moored vessel.

Special effort is invested to achieve symmetrical forms of equation sets for static and dynamic analysis. These symmetrical forms enable easier numerical implementation utilizing classical FEM codes.

Comparison between the improved model and the current equivalent model is done, see **Case study I**. The single mooring line that can be analytically described was a base for comparison. The improved model achieved better matching with analytical results. Satisfactory stability and results of the improved model are found in the coupled dynamic analysis of a moored deepwater spar, see **Case study II**. Therefore, the mooring line model from this paper is a good cornerstone for future research.

References

[1] NORDGEN, R. P.: "On Computation of the Motion of Elastic Rod", Journal of Applied Mechanics, 41(1974), p. 777-780.
[2] GARRETT, D. L.: "Dynamic Analysis of Slender Rods", Journal of Energy Resources Technology, 104(1982), p. 302-307.
[3] Proceedings of The 16th International Ship and Offshore Structures Congress; Report of Committee 1.2, Loads; Editors: FREIZE, P. A., SHENOI, R. A.; Southampton 2006.
[4] TAHAR, A., KIM. M. H.: "Hull/Mooring/Riser Coupled Dynamic Analysis and Sensitivity Study of Tanker-based FPSO", Applied Ocean Research 25:6, p. 367-382; 2003.
[5] GARRETT, D. L.: "Coupled Analysis of Floating Production System", Ocean Engineering, 32:7, p. 802-816; 2005.
[6] KIM, M. H., KOO, B. J., MERCIER, R. M., WARD, E. G.: "Vessel/Mooring/Riser Coupled Dynamic Analysis of

Turret-moored FPSO Compared with OTRC Experiment", Ocean Engineering, 32:14-15, p. 1780-1802; 2005.
[7] FERNANDES, A. C., Del VECCHIO, C. J. M., CASTRO, G.A.V.: "Mechanical Properties of Polyester Mooring Cables", International Journal of Offshore and Polar Engineering; Vol. 9 No 3, 1999.
[8] TJAVARAS, A. A., ZHU, Q., LIU, Y., TRIANTAFYLLOU, M. S., YUE, D. K. P.: "The Mechanics of Highly-extensible Cabels", Journal of Sound and Vibration (1998) 213(4), p. 709-737.
[9] TAHAR, A., KIM, M. H.: "Coupled Dynamic Analysis of Floating Structures with Polyester Mooring Lines", Ocean Engineering, 35: 17-18, p. 1676-1685; 2008.
[10] KREYSZIG, E.: "Advanced Engineering Mathematics", Seventh edition, John Wiley & Sons, Inc., New York 1993.
[11] SPARKS, C. P.: "Fundamentals of Marine Riser Mechanics - Basic Principles and Simplified Analyses", Penwell, Tulsa, Oklahoma, 2007.
[12] API RP 16Q, "Recommended Practice for Design, Selection, Operation and Maintenance of Marine Drilling Riser Systems"; American Petroleum Institute, Washington DC, 1993.
[13] CHEN, X., ZHANG, J., JOHNSON, P., IRANI, M.: "Dynamic Analysis of Mooring Lines with Inserted Springs", Applied Ocean Research, 23, p. 277-288, 2001.
[14] ARCANDRA, "Hull / Mooring / Riser Coupled Dynamic Analysis of a Deepwater Floating Platform with Polyester Lines", Dissertation, Texas A&M University, 2001.
[15] ZIENKIEWICZ, O.C., TAYLOR, R.L.: "The finite element method for solid and structural mechanics", McGraw-Hill, London, 2005.
[16] CUMMINS, W. E.: "The Impulse Response Function and Ship Motions", Schiffstechnik, 1962.
[17] OGILVIE, T. F.: "Recent Progress toward the Understanding and Prediction of Ship Motions", Proceedings of 5th Symp. on Naval Hydrodynamics, 2-128, 1964.
[18] Bureau Veritas, "Hydrostar for Experts, v6.11 - User Manual", 2010.
[19] CHEN, X. B., REZENDE. F.: "Computations of Low-Frequency Wave Loading", The 23rd International Workshop on Water Waves and Floating Bodies, Jeju, Korea, 2008.
[20] API RP 2A, "Recommended Practice for Planning and Constructing Fixed Offshore Platforms - Load and Resistance Factor Design" American Petroleum Institute, Washington DC, 1993.

Appendix A

Shape functions

Hermite polynomials are used for shape functions A_l and P_m during derivation of FEM, as follows [14]

$$\begin{aligned} A_1 &= 1-3\xi^2+2\xi^3 \\ A_2 &= L\left(\xi-2\xi^2+\xi^3\right) \\ A_3 &= 3\xi^2-2\xi^3 \\ A_4 &= L\left(-\xi^2+\xi^3\right) \end{aligned} \tag{A1}$$

and

$$\begin{aligned} P_1 &= 1-3\xi+2\xi^2 \\ P_2 &= 4\xi(1-\xi) \\ P_3 &= \xi(2\xi-1) \end{aligned} \tag{A2}$$

with

$$\xi = \frac{s}{L}. \tag{A3}$$

where L is length of finite element.

Appendix B

Loads on a moored floating object

Wave loads of the first order on the floating object are defined by linear transfer function (LTF), according to [18]

$$\left\{F_W^{(1)}(t)\right\} = R\left\{\sum_{j=1}^{N}\mathbf{a}_j\left\{f^{(1)}\right\}_j \mathrm{e}^{-i\omega_j t}\right\}, \tag{B1}$$

where

i – imaginary unit
e^x – exponential function of x
$R\{\}$ – denotes real part of complex quantity
$\left\{f^{(1)}\right\}_j$ – linear transfer function (LTF) for wave loads of the first order
$\mathbf{a}_j$ – complex amplitude of a wave component
ω_j – frequency of a wave component
N – total number of wave components.

Wave loads of the second order are defined using quadratic transfer function (QTF), according to [18] and [19]

$$\left\{F_W^{(2)}(t)\right\} = R\left\{\sum_{j=1}^{N}\sum_{k=1}^{N}\left\{f^{(2)}\right\}_{jk}\mathbf{a}_j\,\mathbf{a}_k^*\,\mathrm{e}^{-i(\omega_j-\omega_k)t}\right\}, \tag{B2}$$

where

$\left\{f^{(2)}\right\}_{jk}$ – quadratic transfer function (QTF) for wave loads of the second order
$\mathbf{a}^*$ – complex conjugate of $\mathbf{a}$.

The amplitude of each wave component is determined based on a wave spectrum that describes a sea state

$$\mathbf{a}_j = \mathrm{e}^{i\theta_j}\sqrt{2S_{\eta\eta}(\omega_j)\Delta\omega_j}, \tag{B3}$$

where

$S_{\eta\eta}$ – wave spectrum
θ_j – phase of a wave component (determined on the basis of a random number)
$\Delta\omega_j$ – frequency step size.

Wind load on the hull of a floating object can be calculated using simplified engineering approximation

$$F_{WN} = C_{WN}\,V_{WN}^2, \tag{B4}$$

where

F_{WN} – wind load
C_{WN} – wind load coefficient dependant on the type of floating object and the exposed projected area.

The wind speed is defined on the basis of wind spectrum, see [20].

It can be assumed that the load due a sea current has only constant component. To determine the amount of load the following formula is used

$$F_{CR} = \frac{1}{2} C_{CR}\, \rho V_{CR}^2\, A_{UP}, \tag{B5}$$

where

F_{CR} – sea current load
C_{CR} – coefficient of sea current load (or drag force coefficient)
ρ – density of the sea water
V_{CR} – speed of the sea current
A_{UP} – underwater projected area.

Appendix C

Analytical solution for the case study I

The analytical solution of a single mooring line in the **Case study I** (see Fig. 7) is based on a classical equation for rod deformation

$$AE \frac{\mathrm{d}u}{\mathrm{d}x} = N, \tag{C1}$$

where

AE – axial stiffness of a rod
u – longitudinal displacement
x – local longitudinal coordinate axis
N – cross-sectional force.

Eq. (C1) is used for each segment of the mooring line. The origin of the local coordinate system is set up at the end of the segment that is closer to the seabed. In the case of a single mooring line the cross-section force N and the real tension force T_R are the same.

Since the segments of the mooring line are vertical, the force T_R is simply formed for each segment in the local coordinate system

$$T_R(x) = R + q_{E1} x \text{ , for Segment 1} \tag{C2}$$

$$T_R(x) = \left(R + q_{E1} l_1\right) + q_{E2}\, x - \rho g \left(l_2 + l_3 - x\right) A \text{ , for Segment 2} \tag{C3}$$

$$T_R(x) = \left(R + q_{E1} l_1 + q_{E2} l_2\right) + q_{E3}\, x, \text{ , for Segment 3} \tag{C4}$$

with

$$R = F_V - q_{E1} l_1 - q_{E2} l_2 - q_{E3} l_3 \tag{C5}$$

where R is reaction force at the seabed; q_{E1}, q_{E2} and q_{E3} are effective distributed loads of segments, see (30); l_1, l_2 and l_3 are lengths of segments; F_V is the vertical force on the top of the mooring line which contains initial pretension. During formulation of (C3) for Segment 2 it is necessary to consider (24). For the nonlinear case of polyester rope material axial stiffness is calculated using (29).